Reference: *Biol. Bull.* **227:** 51–60. (August 2014)

Aminoglycoside-Induced Damage in the Statocyst of the Longfin Inshore Squid, *Doryteuthis pealeii*

ALEXANDRA L. SCHARR[1,2,*], T. ARAN MOONEY[1], FELIX E. SCHWEIZER[3,4] AND DARLENE R. KETTEN[1,5,6]

[1]*Biology Department, Woods Hole Oceanographic Institution, Woods Hole, Massachusetts 02543;* [2]*Stanford University School of Medicine, Palo Alto, California 94305;* [3]*Marine Biological Laboratory, Woods Hole, Massachusetts 02543;* [4]*Department of Neurobiology, David Geffen School of Medicine, University of California, Los Angeles, California 90095;* [5]*Harvard Medical School, Boston, Massachusetts 02114; and* [6]*Curtin University, Perth, Western Australia 6845, Australia*

Abstract. Squid are a significant component of the marine biomass and are a long-established model organism in experimental neurophysiology. The squid statocyst senses linear and angular acceleration and is the best candidate for mediating squid auditory responses, but its physiology and morphology are rarely studied. The statocyst contains mechano-sensitive hair cells that resemble hair cells in the vestibular and auditory systems of other animals. We examined whether squid statocyst hair cells are sensitive to aminoglycosides, a group of antibiotics that are ototoxic in fish, birds, and mammals. To assess aminoglycoside-induced damage, we used immunofluorescent methods to image the major cell types in the statocyst of longfin squid (*Doryteuthis pealeii*). Statocysts of live, anesthetized squid were injected with either a buffered saline solution or neomycin at concentrations ranging from 0.05 to 3.0 mmol l^{-1}. The statocyst hair cells of the macula statica princeps were examined 5 h post-treatment. Anti-acetylated tubulin staining showed no morphological differences between the hair cells of saline-injected and non-injected statocysts. The hair cell bundles of the macula statica princeps in aminoglycoside-injected statocysts were either missing or damaged, with the amount of damage being dose-dependent. The proportion of missing hair cells did not increase at the same rate as damaged cells, suggesting that neomycin treatment affects hair cells in a nonlethal manner. These experiments provide a reliable method for imaging squid hair cells. Further, aminoglycosides can be used to induce hair cell damage in a primary sensory area of the statocyst of squid. Such results support further studies on loss of hearing and balance in squid.

Received 2 December 2013; accepted 16 May 2014.

* To whom correspondence should be addressed, at Stanford University School of Medicine, Palo Alto, CA 94305. E-mail: scharr@stanford.edu

Introduction

The squid statocyst and its sensory hair cells share many characteristics with vertebrate vestibular systems yet maintain intriguing morphological differences, despite the functional commonalities of the two systems (Dilly *et al.*, 1975; Dilly, 1976; Stephens and Young, 1982). For example, squid have cartilaginous anticristae and hamuli that protrude into the statocyst cavity and direct the flow of endolymph over cristae ridges, the strips of sensory epithelia that are aligned in three orthogonal planes (Stephens and Young, 1978). A gelatinous and sail-like cupula covering the ridge bends under the flow of endolymph as a squid rotates, activating six rows of underlying, polarized, ciliated, mechanosensory cells, also known as hair cells, thereby encoding angular acceleration (Budelmann *et al.*, 1987; Young, 1989). The gravity receptor system consists of three hair-cell-dense maculae on the anterior and medial walls of the cavity. The receptors also contain pebble-like statoconia which, like most amphibian and bony fish otoconia, are composed of aragonite crystals. This is unlike mammalian and some fish otoconia that are composed of a calcite crystal form of calcium carbonate (Dilly, 1976). Squid statoconia cover the superior and inferior maculae, and a single statolith, similar to an otolith, covers the largest, most anterior macula. The hair cells of the maculae are also polarized (Budelmann, 1979). In addition to linear and angular acceleration, squid can detect, and be affected by, the particle

motion component of sound, with the statocyst effectively acting as an accelerometer and a simple auditory system (Packard *et al.*, 1990; Budelmann *et al.*, 1992; Mooney *et al.*, 2010).

Recent research supports earlier hypotheses of sound detection by squid (Hanlon and Budelmann, 1987; Mooney *et al.*, 2010, 2012; Kaifu *et al.*, 2011). Sound detection is thought to be mediated by the squid statocyst, an evolutionarily ancient sensory system that is primarily a gravity detector and accelerometer (Budelmann, 1990). The statocyst is analogous to the fish otolith system (Fay, 1974) and, to some extent, may share functions of the inner ear hair cells of higher vertebrates (Yost, 1994). Because squid are now considered to respond to some acoustic components, there is concern that increases in ocean noise may damage statocyst hair cells and impact their hearing (Packard *et al.*, 1990; Budelmann *et al.*, 1992; Kaifu *et al.*, 2008; Hu *et al.*, 2009; André *et al.*, 2011; Mooney *et al.*, 2012; Solé *et al.*, 2013). Additionally, squid have been a model species in physiology and neuroscience since the classic experiments by Hodgkin and Huxley on the nature of the action potential (Hodgkin and Huxley, 1945, 1952), and their use is growing in other areas such as the study of camouflage and animal-bacterial symbioses (Hanlon, 2007; Lee *et al.*, 2009). Therefore, they may be useful candidates for both basic and comparative vestibular and auditory research**.**

The mechanoreceptive hair cells in the squid statocyst have specific characteristics useful for comparative neurobiological and evolutionary study. Most vertebrate vestibular hair cells are topped with a bundle of stereocilia of increasing length and extended kinocilium and a bipolarity with maximum activation when deflected toward the kinocilium. Squid statocyst hair cells, by contrast, have a bundle of cilia of the same length inclined toward the cell surface (Burighel *et al.*, 2011). In the octopus, hair cells are maximally activated when the cilia are deflected away from the incline (Budelmann and Williamson, 1994).

Aminoglycosides can be toxic to hair cells in many species (Brignull *et al.*, 2009), but this has not yet been tested in cephalopods. Aminoglycosides are thought to enter hair cells through the transduction channel (Marcotti *et al.*, 2005). Investigating possible aminoglycoside toxicity on hair cells of cephalopods would provide information on the similarities or differences between the transduction channels. For example, aminoglycoside toxicity in cephalopods could indicate similarities in the transduction channel in cephalopods and vertebrates, despite the cephalopod bundle being entirely tubulin as opposed to actin-based. Also, vertebrate hair cells are all secondary sensory cells that communicate with the central nervous system through primary afferent neurons. Invertebrate hair cells are typically primary sensory cells with an action-potential-propagating axon. Unlike the simpler marine invertebrate vestibular systems like that of nautilus, squid statocysts contain both primary and secondary sensory cells (Williamson, 1990; Burighel *et al.,* 2011). This offers a unique opportunity to study and compare, at the cellular level, two types of mechanosensation in the same sensory epithelium.

Unlike vertebrate vestibular systems, which incorporate or are encased in bone, the squid statocyst capsule is cartilaginous and therefore easy to access (Stephens and Young, 1982; Budelmann, 1990). The sensory epithelia are robust, surviving for hours after dissection without complex culture media (Budelmann and Williamson, 1994). Despite thorough investigation using classical dissection and scanning electron microscopy studies (Budelmann *et al.*, 1973; Dilly, 1976; Stephens and Young, 1982; Solé *et al.*, 2013), the statocyst and other systems of cephalopods are just beginning to be explored with advanced imaging and electrophysiological techniques. Developing molecular techniques is both appropriate and timely given the advances in techniques and applications for squid as a model system.

To this end, and focusing on the squid vestibular system, we developed a fluorescent immunohistochemical procedure to stain the major cell types in the sensory epithelia of the squid statocyst, laying the groundwork for exploration of the squid system using diverse molecular and molecular imaging techniques. In addition to imaging these structures using fluorescent immunohistochemistry, we investigated their vulnerability to pharmaceutical and chemical toxicity.

Materials and Methods

Animals

Adult longfin inshore squid (*Doryteuthis pealeii* (Leseur, 1821); formerly *Loligo pealeii*) were collected in Vineyard Sound, near Woods Hole, Massachusetts, *via* trawler boat. Animals exhibiting normal swimming and coloration patterns (Hanlon and Messenger, 1996) were hand-selected from the boat and transported in aerated seawater in coolers to the Woods Hole Oceanographic Institution, Woods Hole, Massachusetts, where they were housed in tanks of filtered seawater. Seventy squid, with a mean wet weight of 76.1 $\pm$ 33.3 g and a mean mantle length of 13.6 $\pm$ 3.8 cm, were used over the course of the experiments.

Dissection, tissue treatment, and immunohistochemical analyses

The initial goal of these tests was to develop a robust immunofluorescent staining method to image major cell types in the squid statocyst. To access the statocyst, squid were decapitated without prior anesthesia. To avoid damaging the statocyst during decapitation, care was taken to make the incision sufficiently close to the mantle (Fig. 1) by holding back the funnel and decapitating where the funnel attaches to the body, thus exposing the posterior walls of the

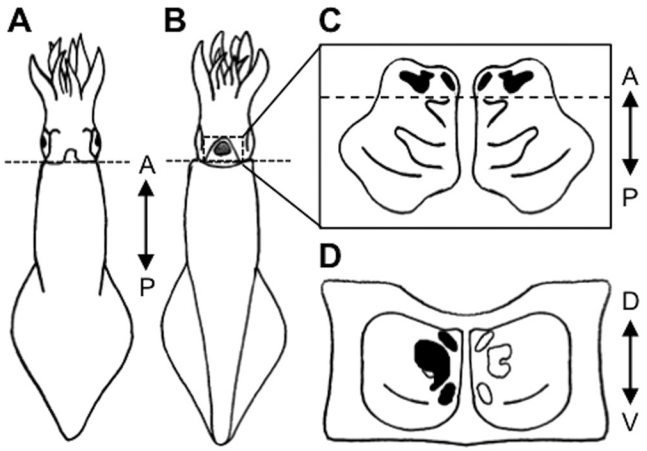

Figure 1. Diagram of statocyst location, dissection procedure, and sensory epithelia. Arrows indicate orientation of squid and statocyst: A for anterior, P for posterior, D for dorsal, and V for ventral. (A) Dorsal view of squid. Dotted line shows dissection location. (B) Ventral view of squid. Dotted line represents dissection location. Dotted box shows location of the statocyst cavity, under the funnel and between the eyes. (C) Ventral view of intact statocyst with funnel and overlying tissue removed. Statolith (larger black area) and statoconia (smaller black area) are visible at the far anterior end of the cavity. Dotted line indicates dissection incision to open the statocyst. (D) Anterior view of the opened statocyst cavity. Left cavity shows locations of statolith (central; black) and statoconia (superior and inferior; black, top and bottom respectively). Right cavity outlines sensory epithelia underneath statolith and statoconia. These are, from dorsal to ventral, the macula neglecta anterior, the macula statica princeps, and the macula neglecta posterior.

bilateral statocysts. The statocysts are located between the eyes and, when accessed in this way, appear as two small, round cavities. The statocysts and surrounding cartilage were then extracted as a block with three additional incisions, two laterally and one anteriorly. A generous amount of surrounding tissue was initially included and used to stabilize the statocyst during the dissection of the sensory epithelium. Four to ten statocysts were prepared during each experimental session. The intact statocysts were then placed in 24-well plates and submerged in fixative solution (4% paraformaldehyde in filtered seawater; EMS, Hatfield, PA) overnight at room temperature (23 °C). This was an experientially determined time period, based on consistent dissection and staining of the delicate sensory epithelium with little mechanical damage resulting from the tissue preparation procedures.

The fixed statocysts were then rinsed three times for 5 min in PBS (0.1 mol l^{-1} phosphate buffered saline; Sigma Aldrich, St. Louis, MO); aligned ventral side up, posterior end closest to the experimenter; and held by a bulldog clamp attached to tissue adjacent to the dorsal side of the statocyst, being careful to avoid clamping the statocyst itself. Forceps were used to tease away the tissue on the ventral side of the statocyst until the statolith could be seen with the naked eye through the cartilage cover and primary statocyst tissue. The macula statica princeps of each statocyst was exposed by carefully reducing the anterior wall of the statocyst with a scalpel, approaching the statolith as closely as possible without opening the cavity. The posterior end of the cavity was then dissected away by making an incision as close to the statolith as possible (Fig. 1C) without disturbing it, which might damage the underlying epithelium, and thus obtaining a tissue section about 1–2 mm thick (Fig. 1D).

Indirect immunohistochemistry was used to image and allow morphological characterization of the hair cells. The tissue sections were rinsed three times for 5 min in BSA/PBST (1% bovine serum albumin and 0.1% Triton X-100 in PBS; Sigma Aldrich, St. Louis, MO). If the statolith remained on the sensory epithelium, it was gently removed with jets of BSA/PBST from a micropipette. The sections were incubated in 5% normal goat serum in BSA/PBST for 1 h and then incubated overnight in mouse anti-acetylated tubulin IgG (1:1000 in PBST; #T7451, Sigma, St. Louis, MO). Sections were rinsed four times for 10 min in BSA/PBST and then incubated, protected from light, for 1 h in CF594-labeled goat anti-mouse IgG antibody (1:400 in PBST; #20110, Biotium, Hayward, CA). Sections were then rinsed three times for 5 min in PBS and stored, protected from light. Sections were immobilized on a glass slide using adhesive spacers and analyzed under an epifluorescence Zeiss Axio Imager.A2 microscope (Carl Zeiss Microimaging, Thornwood, NY) equipped with a fluorescence filter set (excitation BP 565/30, barrier FT 858 and emission BP620/60) using a 20×, 1.3 NA Plan Neofluar lens. Images were taken with an AxioCam MRc digital microscope camera and analyzed using AxioVision (Carl Zeiss Microimaging, Thornwood, NY) and ImageJ ver. 1.44 software (http://imagej.nih.gov/ij).

Aminoglycoside exposures

Squid were removed one at a time from the holding tank and sedated in a bath of filtered seawater supplemented with 150 mmol l^{-1} $MgCl_2$ (Mooney *et al.*, 2010) before transfer to a 10–l plastic bin (30 cm × 18 cm × 12 cm) filled with filtered seawater (14 °C) on the experimental table adjacent to the holding tank.

The statocyst cavities of experimental squid were injected with neomycin (Sigma-Aldrich, St. Louis, MO) in 0.5-μm filtered seawater at concentrations of 0.00 (control condition), 0.05, 0.10, 0.80, 1.6, or 3.0 mmol l^{-1}. Each squid was held by hand, submerged in filtered seawater ventral side up, while the ventral wall of the statocyst was exposed by manually folding back the funnel. The posterior end of the statocyst cavity was then carefully injected with 10 μl of solution using a 50-μl syringe with a 31-gauge needle. All solutions were colored with a nontoxic blue dye (Brilliant Blue FCF, E133) at a concentration of 0.5%, which made it

possible to visually determine whether the statocyst cavity was completely filled. Non-injected squid served as additional controls.

Individual squid were then placed in separate 20 cm × 20 cm mesh bags in order to identify them later and suspended in the holding tank to recover from the sedation, which lasted about 20 min. After 5 h, the squid were removed from the bags and transferred to the experimental table, where each was decapitated without prior anesthesia and the intact statocyst was removed. The tissue was prepared and processed for immunohistochemistry as described above.

Quantification and statistical analysis

Hair cell damage was determined by classifying the hair cells as intact, damaged, or missing in a 226 μm × 168 μm area of the macula statica princeps. This region of interest represents about 20% of the epithelium and was chosen because it could be located consistently and, due to its far anterior location, was least likely to sustain accidental damage from treatment and tissue preparation. Hair cells were classified as intact if the kinociliary bundle was undamaged—that is, if the kinocilia were aligned and the bundle was complete and brightly stained by the indirect fluorescent immunohistochemistry previously described. Hair cells were classified as damaged if the bundle was splayed or partially or entirely missing. Hair cells were classified as missing if there was no tubulin labeling where a cell body would be found in an untreated statocyst. However, since we did not directly test the presence or absence of intact cell bodies with, for example, a nuclear stain, we cannot rule out the possibility that our "missing" hair cells completely lacked their kinociliary bundles. The counts were converted to a percentage of total hair cells in the region of interest in each epithelium for final analysis.

Statistical tests were performed using R software ver. 2.15.0 (R Foundation for Statistical Computing, Vienna, Austria), and each statocyst cavity was treated as statistically independent because dye always remained in the one statocyst cavity, never leaking into other structures or the cartilaginous wall. The total number of possible hair cell bundles (the sum of those intact, damaged, and missing labeling) in each image was tested for normality and homogeneity of variance using Bartlett and Shapiro tests, respectively, and then tested for differences between conditions with a one-way analysis of variance (ANOVA). Data from non-injected control and 10-μl saline-injected statocysts were tested for normality and homogeneity of variance using Bartlett and Shapiro tests, respectively, and then compared using a two-tailed Student's *t*-test to determine the effect of the injection alone on hair cell condition. To determine the effect of neomycin concentration on statocyst hair cell condition, data from saline- and neomycin-injected statocysts were compared using one-way ANOVA with Welch's correction for non-homogeneity of variance, and *post hoc* pairwise comparisons using nonparametric Mann-Whitney-Wilcoxon tests with Bonferroni correction, as well as Spearman's rank correlations.

Results

Staining

To visualize hair cells in the squid statocyst, we chose an antibody directed against acetylated alpha tubulin since acetylation is a common post-translational modification in stable microtubules, which make up kinocilia, and this antigen recognizes alpha tubulin in many species (Steyger *et al*., 1989; Perdiz *et al.*, 2011). This antibody was visualized using a secondary, CF594-labeled, antibody, and bright and selective staining of cilia bundles was observed throughout the statocyst (Figs. 2, 3A). The antibody also marked, although less brightly, hair cell bodies, supporting cells, and primary afferent neurons (Figs. 2B, 3).

The kinociliary bundles of the three maculae were brightly stained. Due to its anterior location and relatively flat structure, the macula statica princeps was the best-visualized sensory epithelium (Figs. 2A, 4). Kinocilia of cells in the macula statica princeps were arranged in a semicircular pattern radiating from a dorsal midpoint. The kinocilia are arranged in one continuous row per hair cell, which suggests response polarity and is consistent with a standard pattern for healthy hair cells in the squid statocyst (Budelmann *et al.*, 1973). At higher magnifications individual kinocilia were visible (Figs. 2D, 4, and 5). All the hair cells of the macula are morphologically similar, with dense, regular, brush-like kinociliary bundles.

The crista ridge, particularly the crista transversalis anterior and the crista longitudinalis, were also robustly stained with this procedure (Figs. 2B, 2C, 2D, and 3A). The ridge consists of six rows of hair cells. All hair cells of a row are morphologically similar to each other, but the rows are not identical. In the crista transversalis anterior, the most anterior row of hair cells are larger, spaced about one cell length apart, with somewhat splayed kinociliary bundles. The two most posterior rows of hair cells, which are also the most visible in this preparation, are tightly packed, with dense, aligned, brush-like kinociliary bundles.

Many ciliated cells are associated with the crista ridge, where they are more densely packed, becoming sparser with distance from the ridge (Fig. 3A). However, these non-crista intermacular hair cells, all with similar morphologies and tuft-like kinociliary bundles, are found on all walls of the statocyst cavity. Figure 3B shows the cell bodies of three such hair cells located in the statocyst wall laterally from the macula statica princeps. The kinociliary bundles of these hair cells are long and thin (Fig. 3A).

Neuronal cell bodies associated with the crista ridge and their axons were also visible (Fig. 3C, 3D). The largest

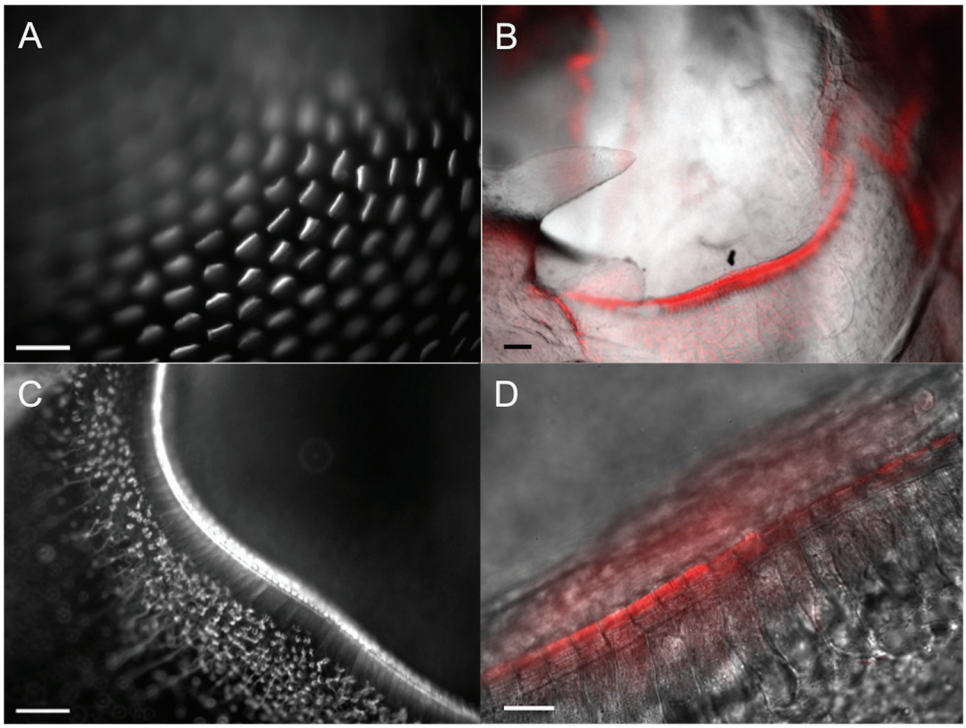

Figure 2. Major cell types of the squid statocyst visualized using anti-acetylated tubulin and CF495. (A) Kinocilary bundles of hair cells of the macula statica princeps are arranged in concentric rows and brightly stained. Bar is 20 μm. (B) Anterior view of a crista ridge. The hair cells, surrounding ciliated cells, and underlying neurons are colored red. The statocyst wall and cartilaginous projections (*i.e.*, on the left) are visible through unfiltered white light. Bar is 100 μm. (C) Anterior view of a crista ridge, cupula removed. Hair cell bundles are most brightly stained and hair cell bodies are visible as elongate, aligned structures radiating below the kinocilia. Underlying primary neurons and surrounding ciliated cells are also visible. Bar is 100 μm. (D) Crista ridge visualized through fluorescently labeled tubulin, overlaying a DIC image. Tubulin brightly labels kinociliary bundles on the cell surfaces. Bar is 20 μm.

neuronal cell bodies were located farther from the crista ridge, about where the intermacular hair cells became sparser. The neurons were located under the intermacular hair cells and the thick axons that project toward the crista ridge. Dendrites were not visualized with this protocol.

Neomycin treatment

The total number of possible hair cell bundles did not differ among groups [one-way ANOVA; $F(1, 58) = 0.95$, $P = 0.33$]. Non-injected and saline-injected controls were indistinguishable and showed minimal damage, with few missing hair cells (Fig. 4A). No significant difference in the percentages of intact hair cells in the regions of interest was found between saline-injected controls (96% $\pm$ 2.0%, $n = 11$) and non-injected controls (97% $\pm$ 2.1%, $n = 10$): Welch two-sample t-test, $t = 0.86$, df = 19, $P = 0.40$. As neomycin exposure concentrations increased, damaged and missing kinocilia were often observed (Figs. 4B, 5A *vs.* 5B). Kinocilia were splayed or absent, leaving only the cuticular plate visible. Some labeling of hair cells was occasionally missing, leaving gaps where labeled kinocilia would normally be found (Fig. 5C).

The variances of potentially impacted hair cells in non-injected animals, saline-injected controls, and 0.05 mmol l^{-1}-injected animals were low and did not differ substantially. However, standard deviations increased substantially for exposures of 0.1 mmol l^{-1} and higher, suggesting that impact incidence increased with exposure concentrations.

Overall, increasing the neomycin concentration in treatment conditions correlated with decreasing percentages of intact hair cells, increasing percentages of damaged hair cells, and increasing percentages of missing hair cells in the region of interest (Fig. 6; Table 1). Multiple one-way analysis of variance tests (ANOVAs) with Welch's correction for non-homogeneity were conducted to compare the effect of neomycin treatment on the percentages of hair cells in the region of interest that were intact, damaged, and missing (Table 1). Among neomycin treatment groups, there were significant differences in the mean percentages of hair cells that were intact [one-way analysis of means; $F(1, 58) = 74.4$, $P < 0.001$)]. A pairwise comparison using Wilcoxon

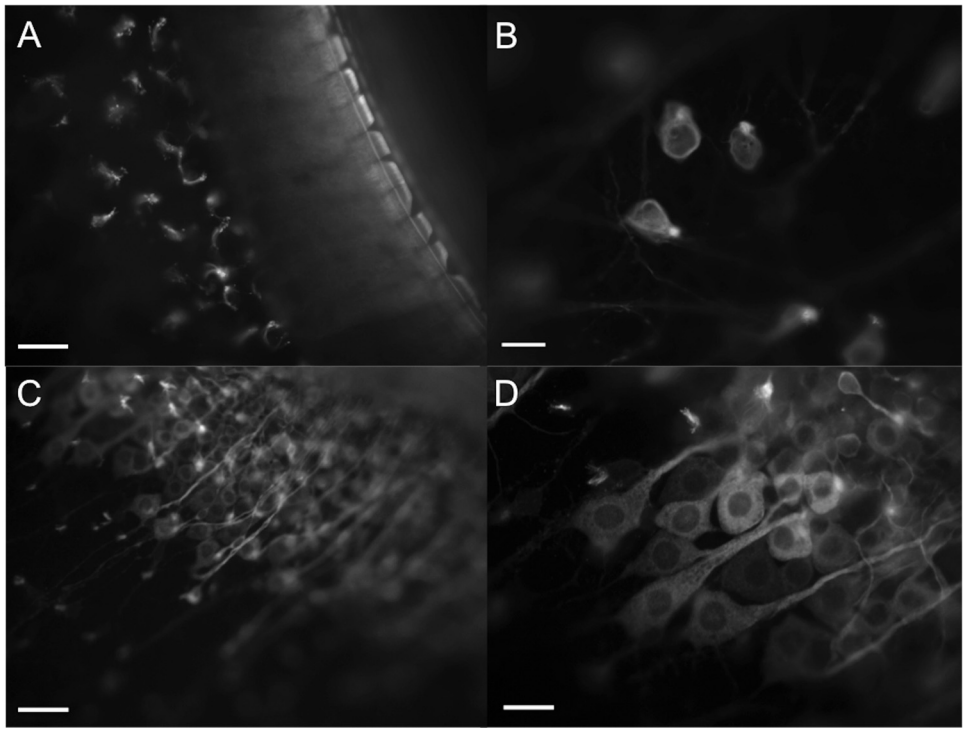

Figure 3. Major cell types of the squid statocyst, focusing on the crista ridge and surrounding tissue, visualized using anti-acetylated tubulin and CF495. (A) Kinociliary bundles (brightly stained) of ciliated cells near the crista ridge, and the first row of hair cells (underneath each kinociliary bundle) in the crista ridge. Bar is 20 μm. (B) Ciliated cells found in the intermacular space. Though most densely packed near the crista ridge, they are also found in looser aggregations between the crista ridge and statolith/statoconia systems. Bar is 20 μm. (C) Axons of neurons associated with the crista ridge. Bar is 80 μm. (D) Soma of neurons associated with the crista ridge. Bar is 20 μm.

rank sum test showed that there were significant differences between most concentration groups ($P < 0.01$; see Fig. 6 for exceptions). There were significant differences in the mean percentages of hair cells that were damaged [one-way ANOM; $F(1, 58) = 64.8$, $P < 0.001$)]. These differences were common to most concentration groups ($P < 0.05$; see Fig. 6 for exceptions).There were also significant differences in the mean percentages of hair cells that were missing [one-way ANOVA; $F(1, 58) = 5.10$, $P < 0.05$)]; however, these differences were only significant between 0 and 3.0 mmol l^{-1}, and 0.05 and 3.0 mmol l^{-1}.

We tested for a dose-dependent response to neomycin

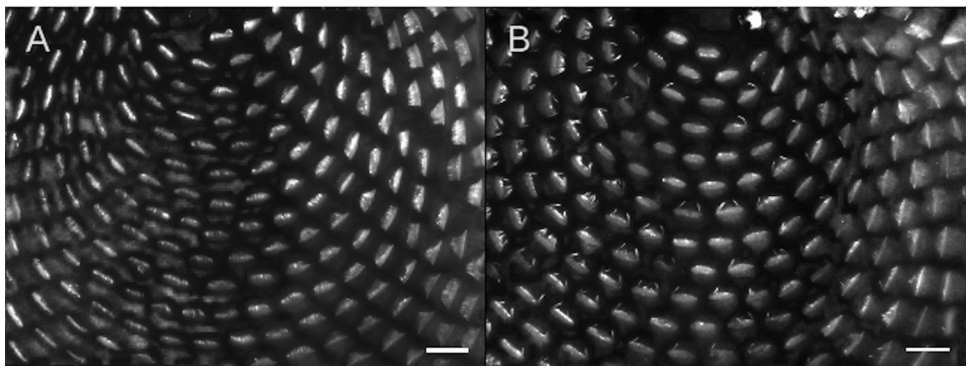

Figure 4. Representative regions of interest (226 μm $\times$ 168 μm) used for quantification of hair cell conditions in different treatment groups. (A) Non-injected control. Kinociliary groups are brush-like and relatively uniform. (B) Statocyst treated with 1.6 mmol l^{-1} neomycin. Some kinociliary groups appear intact, but many are splayed and irregular. See Fig. 5 for detailed scoring examples. Bar is 20 μm.

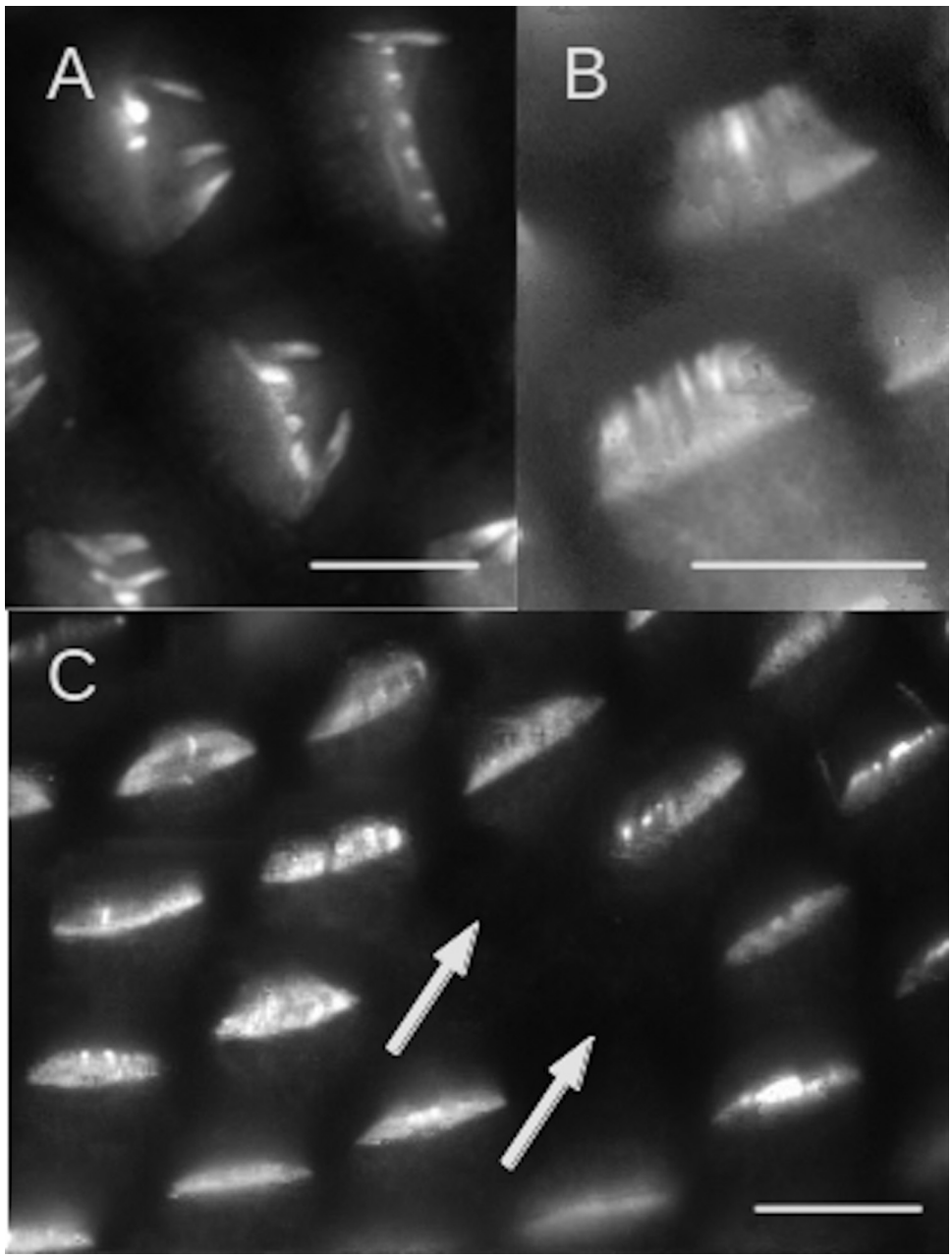

Figure 5. Detailed scoring examples. (A) Example of a hair cell labeled "damaged." Kinocilia are splayed or missing either partially or entirely. Bar is 10 μm. (B) Example of a hair cell labeled "intact." Kinocilia appear intact, are aligned, and often have brightly stained bundle tips. Bar is 10 μm. (C) Examples of hair cells labeled "missing." There is no evidence of tubulin staining in locations, indicated by arrows, where hair cells would normally be found. Bar is 10 μm.

treatment by calculating Spearman's rank correlation for the percentages of hair cells that were intact, damaged, or missing over different treatment groups (Fig. 6). This showed that percentages of intact hair cells decreased with increasing neomycin concentration [$r_s = -0.85$, $P < 0.001$]. Percentages of hair cells that were damaged increased with increasing neomycin concentration [$r_s = 0.85$, $P < 0.001$]. The percentage of hair cells that were missing increased from about 0.5% ± 0.6 % at 0.05 mmol l^{-1} and lower concentrations, to 2.7% ± 16% at 3.0 mmol l^{-1}, with a slight but statistically significant correlation [$r_s = 0.44$, $P < 0.001$].

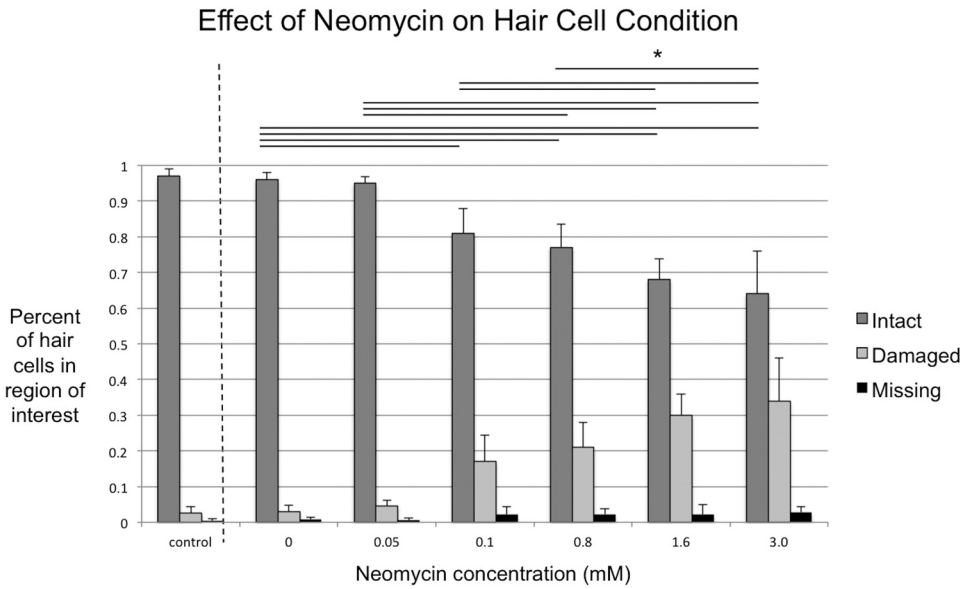

Figure 6. Mean percentages of total hair cells that are missing, damaged, or intact, for all control and experimental conditions. Error bars show standard deviations of the means. Brackets show significant differences between mean percentages of intact hair cells ($P < 0.01$) and between mean percentages of damaged hair cells ($P < 0.05$). For mean percentages of missing hair cells, only differences between 0 and 3.0 mmol l^{-1}, and 0.05 and 3.0 mmol l^{-1} were significant ($P < 0.05$). For details on mean values and variances, see Table 1.

Discussion

These experiments show that neomycin treatment damages the hair cells in one region of the squid statocyst, specifically the kinociliary bundles of the macula statica princeps, in a dose-dependent manner. Increasing the concentration of neomycin in treatment conditions damaged higher proportions of hair cells. Morphologically, intact hair cells maintained their kinociliary bundles, whereas damaged hair cells had hair cell bundles that were splayed, frayed, or missing. Although we focused attention on a subregion of the macula statica princeps, we would expect comparable damage throughout the statocyst. The specific mechanism by which neomycin induces this damage, and whether or not this damage leads to hair cell death, has yet to be determined. In vertebrates, aminoglycosides are thought to enter auditory hair cells through the mechanotransduction channel at the tips of the stereociliary bundles and increase reactive oxygen species within the cell, ultimately leading to apoptosis (Huth *et al.,* 2011). The squid statocyst is primarily a vestibular sensory system, but it also may function as a primitive auditory system (Budelmann, 1979, 1990; Mooney *et al.*, 2010, 2012). Due to the combined vestibular/auditory nature of the statocyst and the heterogeneity of hair cell types in the statocyst, aminoglycoside damage may differ across the epithelium.

The proportion of missing hair cells did not increase at the same rate as damaged hair cell bundles, suggesting that neomycin treatment, at first, might not be causing the hair cells to undergo cell death by either apoptosis or necrosis, but rather that aminoglycoside treatment damages the hair

Table 1

Mean percentage ± standard deviation of total hair cells that are missing, damaged, or intact, in the region of interest for all control and experimental conditions[1]

		Neomycin Concentration (mmol l^{-1})					
	Non-injected control	0.00	0.05	0.10	0.80	1.6	3.0
n	10	11	7	7	8	12	15
% Missing	0.4 ± 0.7	0.8 ± 0.6	0.5 ± 0.6	2.1 ± 2.3	2.2 ± 1.5	2.2 ± 2.7	2.7 ± 1.6
% Damaged	2.6 ± 1.7	3.0 ± 1.7	4.5 ± 1.6	17 ± 7.4	21 ± 7.0	30 ± 6.0	34 ± 12
% Intact	97 ± 2.1	96 ± 2.0	95 ± 1.8	81 ± 6.9	77 ± 6.6	68 ± 5.9	64 ± 12

[1] Significant differences illustrated in Figure 6.

cells in a nonlethal manner at these concentrations. Conversely, it is possible that a higher concentration of aminoglycoside, a longer exposure duration, or both, might cause hair cell death in squid. Though this speculation is not sufficiently supported because this work focused only on the counting of hair cell bundles, squid hair cell death would not be surprising since neomycin toxicity is seen in vertebrates at much lower concentrations of 0.125–0.500 mmol l^{-1} (Harris *et al.*, 2003). However, those studies examined lateral line hair cells, which were bath-exposed to neomycin, as opposed to the encapsulated vestibular system hair cells analyzed in our study, making comparisons with our treatment protocol difficult. Lower concentrations of neomycin treatment (0.8 mmol l^{-1}) do appear to impact statocyst physiological responses in the oval squid, *Sepioteuthis lessoniana,* extinguishing acoustically evoked potentials between 20 and 30 min after methodologically similar injections into the statocyst (Hu *et al.*, 2009). However, Hu *et al*. did not examine morphological changes, and they suggest that the extinction of response may have been due to brain death as opposed to hair cell damage. York and Bartol (2014) also showed that neomycin treatment resulted in *Lolliguncula brevis* squid being preyed upon at higher rates, suggesting the chemical can induce lateral line and sensory damage. Recent studies on the effect of extracellular components on aminoglycoside toxicity also suggest that neomycin affects hair cells differently in high salt concentrations (Coffin *et al.*, 2009).

Demonstrating neomycin-induced kinocilia damage is novel for an invertebrate. The continued development of fluorescent staining techniques, which are faster and less expensive than electron microscopy, should aid researchers in expediting the analysis of hair cell morphology in marine invertebrates. Future work would include addressing the use of fluorescence microscopy for studying hair cell death.

Prior studies have shown the squid statocysts to be key sensory organs that may detect acceleration and can transduce detection of sound stimuli (Budelmann, 1990; Packard *et al.*, 1990; Hu *et al.*, 2009; Mooney *et al.*, 2010)**.** These studies combined with the findings presented here make it attractive to suggest squid hair cells as an invertebrate model system to study hair cell physiology and pharmacology. At the level of the cell, FM1-43, a fluorescent dye that fills functioning vertebrate hair cells and likely enters squid hair cells as well, could be used to infer whether or not the hair cell bundle is transducing—that is, if ions are flowing into the cell through the mechanosensitive ion channels (Nishikawa and Sasaki, 1996)**.** Sharp electrode and whole cell patch clamp electrophysiology have already been used to study the normal functioning of squid hair cells. They have shown that squid hair cells have similar physiological response properties to vertebrate hair cells, despite significant bundle differences, suggesting that the transduction mechanisms share common features (Williamson, 1990, 1995; Budelmann and Williamson, 1994; Chrachri and Williamson, 1997).

In addition, the statocyst is necessary for proper vestibular function, such as the countershading reflex, dorsal light reflex, and compensatory counter rolling of the eyes. Damage to the statocyst disrupts these functions (Schöne and Budelmann, 1970; Colmers *et al.*, 1984; Ferguson and Messenger, 1991; Ferguson *et al.*, 1994; Preuss and Budelmann, 1995; Williamson, 1995). Therefore, behavioral and physiological studies could address whether aminoglycoside treatment damages or extinguishes the statocyst response to vibrations at a fundamental physiological *versus* behavioral level. Using these techniques, auditory and vestibular impairment could be studied after aminoglycoside or other treatment, such as exposure to loud sounds.

Overall, these results show an efficient, relatively inexpensive, and effective way to image squid statocyst hair cells using fluorescent immunohistochemistry to stain tubulin. This technique can be used to morphologically characterize the hair cells of squid. Our data reveal that aminoglycoside antibiotics can induce hair cell damage in an invertebrate, at least in the macula statica region. The exact nature and extent of this damage must be further investigated, but that aminoglycosides may affect non-actin-based mechanotransduction indicates possible physiological and functional similarities between vertebrate and invertebrate hair cells. Overall, the results reveal applications of new techniques to study the statocyst and hair cells of an important model species, which bridges many levels and areas of biological science. Future studies should investigate the specific effects of neomycin and different aminoglycosides and continue to adapt new immunofluorescent labeling techniques to marine invertebrates.

Acknowledgments

This work was supported by Andrew Mellon Award for Independent Research, the Ocean Life Institute, the National Science Foundation, the Office of Naval Research, and the Penzance and John E. and Anne W. Sawyer Endowed Funds. We also thank the MBL Specimens group, including Rhys Probyn and Ed Enos, for providing us with squid, and the 2010 and 2011 Grass Laboratories for sharing both their laboratory space and scientific insights. We are also grateful to Sarah McKay Strobel, Amy Streets, Max Kaplan, and Dr. Jonathan Matsui for their help in completing this project.

Literature Cited

André, M., M. Solé, M. Lenoir, M. Durfort, C. Quero, A. Mas, A. Lombarte, M. van der Schaar, M. López-Bejar, M. Morell, S. Zaugg, and L. Houégnigan. 2011. Low-frequency sounds induce acoustic trauma in cephalopods. *Front. Ecol. Environ.* **9:** 489–493.

Brignull, H. R., D. W. Raible, and J. S. Stone. 2009. Feathers and fins:

non-mammalian models for hair cell regeneration. *Brain Res.* **1277:** 12–23.

Budelmann, B. U. 1979. Hair cell polarization in the gravity receptor systems of the statocysts of the cephalopods *Sepia officinalis* and *Loligo vulgaris. Brain Res.* **160:** 261–270.

Budelmann, B. U. 1990. The statocysts of squid. Pp. 421–439 in *Squid as Experimental Animals,* D. L. Gilbert, W. A. Adelman, and J. M. Arnold, eds. Plenum Press, New York.

Budelmann, B. U., and R. Williamson. 1994. Directional sensitivity of hair cell afferents in the *Octopus* statocyst. *J. Exp. Biol.* **187:** 245–259.

Budelmann, B. U., V. C. Barber, and S. West. 1973. Scanning electron microscopical studies of the arrangements and numbers of hair cells in the statocysts of *Octopus vulgaris, Sepia officinalis* and *Loligo vulgaris. Brain Res.* **56:** 25–41.

Budelmann, B. U., M. Sachse, and M. Staudigl. 1987. The angular acceleration receptor system of the statocyst of *Octopus vulgaris:* morphometry, ultrastructure, and neuronal and synaptic organization. *Philos. Trans. R. Soc. Lond. B Biol. Sci.* **315:** 305–343.

Budelmann, B. U., D. B. Webster, R. R. Fay, and A. N. Popper. 1992. Hearing in non-arthropod invertebrates. Pp. 141–155 in *The Evolutionary Biology of Hearing,* D. B. Webster, R. R. Fay, and A. N. Popper, eds. Springer-Verlag, New York.

Burighel, P., F. Caicci, and L. Manni. 2011. Hair cells in non-vertebrate models: lower chordates and molluscs. *Hear. Res.* **273:** 14–24.

Chrachri, A., and R. Williamson. 1997. Voltage-dependent conductances in cephalopod primary sensory hair cells. *J. Neurophysiol.* **78:** 3125–3132.

Coffin, A. B., K. E. Reinhart, K. N. Owens, D. W. Raible, and E. W. Rubel. 2009. Extracellular divalent cations modulate aminoglycoside-induced hair cell death in the zebrafish lateral line. *Hear. Res.* **253:** 42–51.

Colmers, W. F., R. F. Hixon, R. T. Hanlon, J. W. Forsythe, M. V. Ackerson, M. L. Wiederhold, and W. H. Hulet. 1984. "Spinner" cephalopods: defects of statocyst suprastructures in an invertebrate analogue of the vestibular apparatus. *Cell Tissue Res.* **236:** 505–515.

Dilly, P. N. 1976. The structure of some cephalopod statoliths. *Cell Tissue Res.* **175:** 147–163.

Dilly, P. N., P. R. Stephens, and J. Z. Young. 1975. Receptors in the statocyst of squids. *J. Physiol.* **249:** 59P–61P.

Fay, R. R. 1974. Sound reception and processing in the carp: saccular potentials. *Comp. Biochem. Physiol.* **49A:** 29–42.

Ferguson, G. P., and J. B. Messenger. 1991. A countershading reflex in cephalopods. *Proc. R. Soc. Lond. B Biol. Sci.* **243:** 63–67.

Ferguson, G. P., J. B. Messenger, and B. U. Budelmann. 1994. Gravity and light influence the countershading reflexes of the cuttlefish *Sepia officinalis. J. Exp. Biol.* **191:** 247–256.

Hanlon, R. T. 2007. Cephalopod dynamic camouflage. *Curr. Biol.***17:** R400–R404.

Hanlon, R. T., and B. U. Budelmann. 1987. Why cephalopods are probably not "deaf." *Am. Nat.* **129:** 312–317.

Hanlon, R. T., and J. B. Messenger. 1996. *Cephalopod Behaviour.* Cambridge University Press, Cambridge.

Harris, J. A., A. G. Cheng, L. L. Cunningham, G. MacDonald, D. W. Raible, and E. W. Rubel. 2003. Neomycin-induced hair cell death and rapid regeneration in the lateral line of zebrafish (*Danio rerio*). *J. Assoc. Res. Otolaryngol.* **4:** 219–234.

Hodgkin, A. L., and A. F. Huxley. 1945. Resting and action potentials in single nerve fibres. *J. Physiol.* **104:** 176–195.

Hodgkin, A. L., and A. F. Huxley. 1952. A quantitative description of membrane current and its application to conduction and excitation in nerve. *J. Physiol.* **117:** 500–544.

Hu, M. Y., H. Y. Yan, W.-S. Chung, J.-C. Shiao, and P.-P. Hwang. 2009. Acoustically evoked potentials in two cephalopods inferred using the auditory brainstem response (ABR) approach. *Comp. Biochem. Physiol.* **153A:** 278–283.

Huth, M. E., A. J. Ricci, and A. G. Cheng. 2011. Mechanisms of aminoglycoside ototoxicity and targets of hair cell protection. *Int. J. Otolaryngol.* **2011:** 1–19.

Kaifu, K., T. Akamatsu, and S. Segawa. 2008. Underwater sound detection by cephalopod statocyst. *Fish. Sci.* **74:** 781–786.

Kaifu, K., T. Akamatsu, and S. Segawa. 2011. Preliminary evaluation of underwater sound detection by the cephalopod statocyst using a forced oscillation model. *Acoust. Sci. Technol.* **32:** 255–260.

Lee, P. N., M. J. McFall-Ngai, P. Callaerts, and H. G. de Couet. 2009. The Hawaiian bobtail squid (*Euprymna scolopes*): a model to study the molecular basis of eukaryote-prokaryote mutualism and the development and evolution of morphological novelties in cephalopods. *Cold Spring Harb. Protoc.* **11:** 135.

Marcotti, W., S. M. van Netten, and C. J. Kros. 2005. The aminoglycoside antibiotic dihydrostreptomycin rapidly enters mouse outer hair cells through the mechano-electrical transducer channels. *J. Physiol.* **567:** 505–521.

Mooney, T. A., R. T. Hanlon, J. Christensen-Dalsgaard, P. T. Madsen, D. R. Ketten, and P. E. Nachtigall. 2010. Sound detection by the longfin squid (*Loligo pealeii*) studied with auditory evoked potentials: sensitivity to low-frequency particle motion and not pressure. *J. Exp. Biol.* **213:** 3748–3759.

Mooney, T. A., R. T. Hanlon, and P. T. Madsen. 2012. Potential for sound sensitivity in cephalopods. Pp. 125-128 in *The Effects of Noise on Aquatic Life,* A. N. Popper and A. Hawkins, eds. Springer, New York.

Nishikawa, S., and F. Sasaki. 1996. Internalization of styryl dye FM1-43 in the hair cells of lateral line organs in *Xenopus* larvae. *J. Histochem. Cytochem.* **44:** 733–741.

Packard, A., H. E. Karlsen, and O. Sand. 1990. Low frequency hearing in cephalopods. *J. Comp. Physiol. A* **166:** 501–505.

Perdiz, D., R. Mackeh, C. Poüs, and A. Baillet. 2011. The ins and outs of tubulin acetylation: more than just a post-translational modification? *Cell. Signal.* **23:** 763–771.

Preuss, R., and B. U. Budelmann. 1995. A dorsal light reflex in a squid. *J. Exp. Biol.* **198:**1157–1159.

Rosas-Luis, R., C. A. Salinas-Zavala, V. Koch, P. D. M. Luna, and M. V. Morales-Zárate. 2008. Importance of jumbo squid *Dosidicus gigas* (Orbigny, 1835) in the pelagic ecosystem of the central Gulf of California. *Ecol. Model.* **218:** 149–161.

Schöne, H., and B. U. Budelmann. 1970. Function of the gravity receptor of *Octopus vulgaris. Nature* **226:** 864–865.

Solé, M., M. Lenoir, M. Durfort, M. López-Bejar, A. Lombarte, and M. André. 2013. Ultrastructural damage of *Loligo vulgaris* and *Illex coindetii* statocysts after low frequency sound exposure. *PLoS ONE* **8:** e78825.

Stephens, P. R., and J. Z. Young. 1978. Semicircular canals in squids. *Nature* **271:** 444–445.

Stephens, P. R., and J. Z. Young. 1982. The statocyst of the squid *Loligo. J. Zool. Lond.* **197:** 241–266.

Steyger, P. S., D. N. Furness, C. M. Hackney, and G. P. Richardson, 1989. Tubulin and microtubules in cochlear hair cells: comparative immunocytochemistry and ultrastructure. *Hear. Res.* **42:** 1–16.

Williamson, R. 1990. The responses of primary and secondary sensory hair cells in the squid statocyst to mechanical stimulation. *J. Comp. Physiol. A* **167:** 655–664.

Williamson, R. 1995. Ionic currents in secondary sensory hair cells isolated from the statocysts of squid and cuttlefish. *J. Comp. Physiol. A* **177:** 261–271.

York, C. A., and I. K. Bartol. 2014. Lateral line analogue aids vision in successful predator evasion for brief squid *Lolliguncula brevis*. *J. Exp. Biol.* doi: 10.1242/jeb-102871.

Yost, W. A. 1994. *Fundamentals of Hearing: An Introduction.* Academic Press, New York.

Young, J. Z. 1989. The angular acceleration receptor system of diverse cephalopods. *Philos. Trans. R. Soc. B Biol. Sci.* **325:** 189–237.